Energy Equip. Sys./ Vol. 6/No. 3/Sep. 2018/ 235-246

Energy Equipment and Systems

http://energyequipsys.ut.ac.ir
www.energyequipsys.com

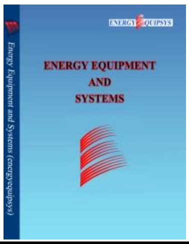

Review Paper

Sensitivity analysis and parameters calculation of PV solar panel based on empirical data and two-diode circuit model

Author

Rahim Moltames [a*]
Mehrdad Boroushaki [a]

[a] Department of Energy Engineering, Energy Systems Engineering, Sharif University of Technology, P.O Box: 14565-114, Azadi Ave, Tehran, Iran

Article history:

Received : 03 February 2018
Accepted : 28 May 2018

ABSTRACT

In this paper, a simple algorithm based on a two-diode circuit model of the solar cell is proposed for calculating different parameters of PV panels. The input parameters required for this algorithm are available from datasheets of the standard PV modules. The values of series and parallel resistances, as well as the recombination factor of Diode 2, are estimated through an iterative solution process. This method is based on maximum power point matching (MPPM) in which the maximum power of PV panel is calculated by the model reaching a minimum error from maximum power proposed in the datasheet. Unlike the other methods, this method is very straightforward and does not require any additional information apart from that of the datasheet. The objective of this paper is to calculate the recombination factor of both diodes in a two-diode PV model, which then leads to further accuracy of the PV model. This novelty in the calculations further improves the accuracy of the model. The simulation is performed in MATLAB, and the effect of altering the temperature of PV cell and level of radiation on the current, voltage, and output power of the PV panel is investigated. The accuracy of the simulation is validated by data extracted from the datasheets of two different PV modules (polycrystalline and monocrystalline).

Keywords: Solar Energy; Photovoltaic; PV Module; Two-Diode Circuit Model.

1. Introduction

The ever increasing energy consumption and limited fossil fuel, globally, necessitates using renewable energies [1]. A PV cell is an important device that can directly convert solar energy into electrical energy. A solar cell employs a semiconductor platform like Si and Ge, including a p-n junction which generates electricity via exposure of the surface to solar energy [2,3].

In order to predict the real behavior of PV under different temperatures and solar intensities as well as to control and evaluate the performance of the cell for developing maximum power point algorithms, it is necessary to calculate the voltage–current and power–voltage characteristic curves [4,5]. The best solution for this purpose is to use a circuit model of the PV cell. In recent years, different models including single-diode, two-diode, three diode, and partial shading have been employed for investigating the real behavior of solar cells. The most important factor which affects the accuracy of simulating the performance of solar cells is the circuit model.

* Corresponding author: Rahim Moltames
Department of Energy Engineering, Energy Systems Engineering, Sharif University of Technology, P.O Box: 14565-114, Azadi Ave, Tehran, Iran
Email: rahim.moltames89@gmail.com

The most common circuit models used for simulations are single-diode and two-diode models. These models are preferred due to certain advantages such as accuracy of obtained parameters, ease of writing code, and extraction of results [6].

One of the most important parameters in photovoltaic cells which also affects the performance of cell is the recombination of the electrons and holes. This can be minimized by using a certain material with a longer lifetime for generated carriers that remove unnecessary impurities [7,8]. A single-diode circuit model is formulated by assuming recombination does not occur in the cell; while in the real PV cell, recombination occurs and its effects, especially in low voltages, are considerable [9]. Accordingly, using a model that can predict the effects of recombination on cell performance will result in a more accurate analysis of cell performance. To this end, a second diode is used in the two-diode circuit model. Using a two-diode circuit model increases the number of parameters used in the model. Different computation methods are proposed for two-diode circuit model. In most of these methods, new structural parameters including diffusion coefficient, minority carrier lifetime, intrinsic carrier density, and other semiconductor parameters are added to the model and the computational burdens are increased. Although all these models are useful, accessing the required parameters of these models through commercial datasheets is impossible [9].

In this paper, a two-diode circuit model of the PV module based on the maximum power point matching (MPPM) algorithm proposed in [9–11] is employed for extracting PV parameters. The advantage of this algorithm is that it does not require any additional data apart from what is available in commercial PV panel datasheets. This paper seeks to determine the recombination factor of both diodes based on a novel algorithm, which then further improves the accuracy of the PV model. The simulation is performed in MATLAB and the effect of altering temperature of the cell and level of radiation on current, voltage, and PV power production is investigated. Finally, the accuracy of the obtained values for voltage, current, and power of the PV is validated with the experimental data of datasheets.

2. Methodology

2.1. Single-diode circuit model

A single-diode model of a PV cell is shown in Fig.1. The PV panel is modeled by a current source and losses caused by conductor and semiconductor connections are modeled with two series and parallel resistances [2,12].

According to Kirchhoff's current law, the general PV current equation in the single-diode model is as follows [13]:

$$I = I_{ph} - I_d - I_p \tag{1}$$

where Iph is the current generated by incident light, Id is the diode current, and Ip is the current of parallel resistance.

The diodes' current is obtained as follows [14]:

$$I_d = I_0\left[\exp\left(\frac{qV}{\alpha kT}\right) - 1\right] \tag{2}$$

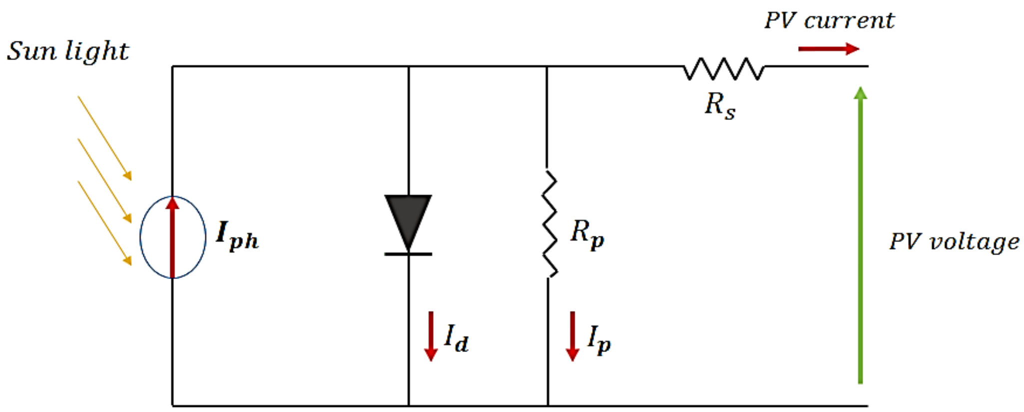

Fig.1. Single-diode model of the PV cell

where I_0 is the saturation current, q is the electron charge $(1.6 \times 10^{-19}\,C)$, V is the PV voltage, α is the diode ideality factor, k is the Boltzmann constant $(1.38 \times 10^{-23}\,J/K)$, and T is the PV temperature.

By applying Eq. (2) to Eq. (1) and considering current passing through parallel resistance, the PV current should be as follows [15]:

$$I = I_{ph} - I_0\left[\exp\left(\frac{q(V+IR_s)}{\alpha kT}\right) - 1\right] - \frac{V+IR_s}{R_p} \tag{3}$$

where R_s is the series resistance and R_p is the parallel resistance.

2.2 Two-diode circuit model

A two-diode circuit model of a PV cell is shown in Fig.2. With constant solar intensity, the relation between current and voltage is obtained as follows:

$$I = I_{ph} - I_{01}\left[\exp\left(\frac{V+IR_s}{\alpha_1 \times V_{T1}}\right) - 1\right] - I_{02}\left[\exp\left(\frac{V+IR_s}{\alpha_2 \times V_{T2}}\right) - 1\right] - \frac{V+IR_s}{R_p} \tag{4}$$

in which, I_{01} is the saturation current for Diode1, I_{02} is the saturation current for Diode 2, α_1 is the Diode1 ideality factor, α_2 is the Diode 2 recombination factor, V_{T1} is the Diode 1 thermal voltage and V_{T2} is the Diode 2 thermal voltage.

According to Shockley's diffusion theory, α_1 should be equal to one. While α_2 might change according to simulation; α_2 affects the curvature of the I–V curve and varying this value may slightly improve the accuracy of model.

Equation (4) cannot be solved directly because the PV current is a function of voltage and current *I=f (I,V)*. Therefore, in order to obtain the voltage–current curve, the numerical solution should be used.

The equation which relates saturation current of the diode to cell temperature is as follows [16,17]:

$$I_0 = I_{0,n}\left(\frac{T}{T_n}\right)^3 \exp\left[\frac{qE_g}{\alpha k}\left(\frac{1}{T_n} - \frac{1}{T}\right)\right] \tag{5}$$

where T_n is the nominal temperature (25°C) and $I_{0,n}$ is the nominal saturation current.

V_T in the Eq. (5) is given by:

$$V_T = \frac{N_s kT}{q} \tag{6}$$

where N_s is the number of series cells.

E_g in Eq. (5) is the energy gap of semiconductor which is 1.12eV for polycrystalline-Si and 1.75eV for Amorphous-Si [18].

In order to calculate the temperature of the cell in Eq. (6), a nominal operating cell temperature (NOCT) is used. According to Eq. (7), the PV cell temperature is related to ambient temperature and solar radiation level [19]:

$$T = T_a + \frac{G}{800} \times (T_{NOCT} - 20) \tag{7}$$

where T_a is the ambient temperature, G is the solar irradiance, and T_{NOCT} is the nominal operating cell temperature which can be accessed in commercial datasheets in centigrade.

Current generated by the cell as a current source is not exactly short-circuit current. In a short circuit, a small amount of current is generated when the cell passes through parallel resistance, thus:

$$I_{ph} = I_{sc} + I_p = I_{sc} + \frac{I_{sc}R_s}{R_p} \tag{8}$$

where I_{sc} is the short-circuit current.

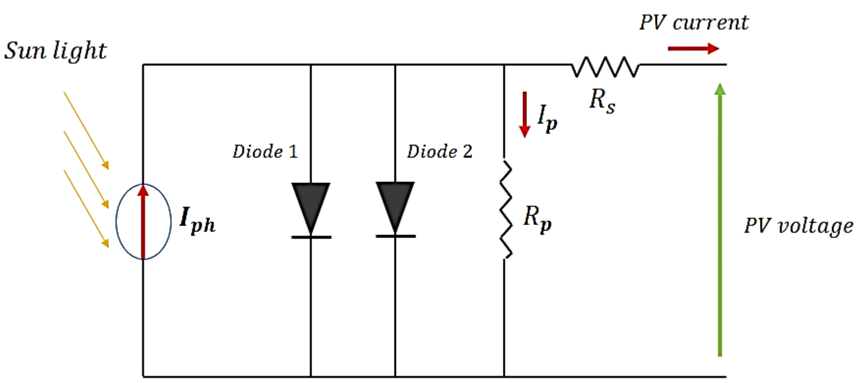

Fig.2. Two-diode model of the PV cell

Simplifying Eq. (8), which relates the cell current to short-circuit current and considering values of series and parallel resistances, it can be rewritten as follows.

$$I_{ph} = I_{sc}\left(\frac{R_p + R_s}{R_p}\right) \tag{9}$$

The nominal saturation current used in Eq. (5) is obtained by Eq. (10):

$$I_{0,n} = \frac{I_{sc,n}}{\exp(V_{oc,n} / \alpha \times V_{T_n}) - 1} \tag{10}$$

where $I_{sc,n}$ is the nominal short-circuit current, $V_{oc,n}$ is the nominal open-circuit voltage, and $V_{T,n}$ is the nominal thermal voltage.

The proposed model for the relationship between saturation current of diode and temperature in Eq. (5) can be improved as follows [10]:

$$I_0 = \frac{I_{sc,n} + k_I (T - T_n)}{\exp(V_{oc,n} + k_V (T - T_n) / \alpha V_T) - 1} \tag{11}$$

where k_I is the short-circuit current coefficient and k_V is the open-circuit voltage coefficient.
Eq. (11) uses voltages and temperature coefficients as can be accessed in commercial datasheets, instead of semiconducting and structural parameters of the cell.

The electrical current of the cell is related to the radiation energy of the sun linearly and its relationship with radiation and temperature is written as follows [20]:

$$I_{ph} = \left[I_{ph,n} + k_I (T - T_n)\right]\frac{G}{G_n} \tag{12}$$

where $I_{ph,n}$ is the nominal current generated by incident light and G_n is the nominal solar irradiance.

For simplification, the saturation currents are considered to be equal in both the diodes [9]:

$$I_{01} = I_{02} = \frac{\left[I_{sc,n} + k_I (T - T_n)\right]}{\exp\left\{\left[V_{oc,n} + k_V (T - T_n)\right]/V_T\right\} - 1} \tag{13}$$

As mentioned before, all the parameters employed in the two-diode model except R_s, R_p, α_1, and α_2 can be accessed from the commercial PV datasheets.

2.3. Maximum Power Point Matching (MPPM) algorithm

The values of $\alpha 1$ and α_2 are assumed to be one and two, respectively. To increase the accuracy of the model, the value of α_2 will be later modified. In order to calculate values of R_s and R_p, the MPPM algorithm is used. According to this algorithm, the model calculates the maximum power of the PV panel based on the minimum error from the maximum power proposed in the datasheet. The maximum power point of a typical PV on the current–voltage curve is shown in Fig.3.

The electrical power at the maximum point is obtained as follows:

$$\begin{aligned} &P_{max,C} \\ &= V_{mp} \\ &\times \left(I_{ph} - I_{01}\left[\exp\left(\frac{V_{mp} + I_{mp}R_s}{\alpha_1 \times V_{T1}}\right) - 1\right]\right. \\ &- I_{02}\left[\exp\left(\frac{V_{mp} + I_{mp}R_s}{\alpha_2 \times V_{T2}}\right) - 1\right] \\ &\left. - \frac{V_{mp} + I_{mp}R_s}{R_p}\right) = P_{max,E} \end{aligned} \tag{14}$$

where $P_{max,C}$ is the calculated peak power, $P_{max,E}$ is the experimental peak power, V_{mp} is the PV voltage at peak power, and I_{mp} is the PV current at peak power.

By solving Eq. (15) for R_p, the following equation is satisfied:

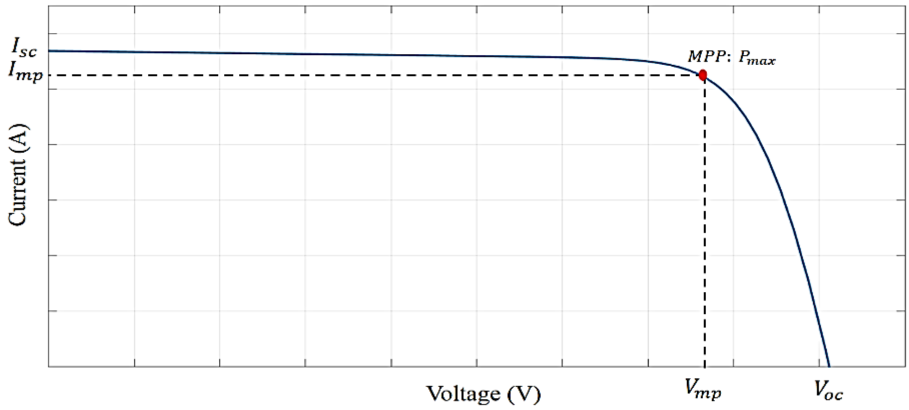

Fig.3. A typical PV current–voltage curve

$$R_p = \frac{V_{mp}\left(V_{mp} + I_{mp}R_s\right)}{\left(V_{mp}\left[I_{ph} - I_{d1,mp} - I_{d2,mp}\right] - P_{\max,E}\right)} \quad (15)$$

in which, current of Diodes 1 and 2 at maximum power point are calculated as follows:

$$I_{d1,mp} = I_{01}\left[\exp\left(\frac{V_{mp} + I_{mp}R_s}{\alpha_1 \times V_{T1}}\right) - 1\right] \quad (16)$$

$$I_{d2,mp} = I_{02}\left[\exp\left(\frac{V_{mp} + I_{mp}R_s}{\alpha_2 \times V_{T2}}\right) - 1\right] \quad (17)$$

By increasing R_s at each iteration, R_p is also increased according to Eq. (15), and both values are used to calculate maximum output power (Eq. 14). R_s varies until maximum output power of the PV ($P_{max,C}$) becomes equal to maximum power presented in the datasheet ($P_{max,E}$). The initial values of series and parallel resistances are given below:

$$R_s = 0\,; \quad (18)$$

$$R_p = \frac{V_{mp}}{I_{sc,n} - I_{mp}} - \frac{V_{oc,n} - V_{mp}}{I_{mp}}$$

The algorithm of this method is shown in Fig.4.

According to the algorithm shown in Fig.4, the parameters of the datasheet including: open-circuit voltage (V_{oc}), short-circuit current (I_{sc}), the voltage at maximum power (V_{mp}), current at the maximum power (I_{mp}), short-circuit-current coefficient (K_I), open-circuit voltage coefficient (K_V) , and experimental power point ($P_{max.E}$) are first entered into the running code. Then, the saturation current of the diodes is calculated according to Eq. (13) at the standard temperature. The only remaining parameters for the calculation of PV current (Eq. (4)) are R_s and R_p. By initializing the series resistance and calculating the parallel resistance, according to Eq. (15), it is possible to calculate the PV current and voltage, simultaneously for different R_s values. The desirable values for R_s and R_p are indicated at the point at which maximum power calculated by the algorithm has a minimum error from maximum power provided by the datasheet. After running the algorithm once, the values of R_s and R_p are obtained and used as constant values in subsequent executions for analyzing sensitivity.

Fill factor (FF) index is one of the most important indices for evaluating the quality of PV cells. This index shows the quadrature of the I–V curve and its value is obtained using the following equation.

$$FF\,(\%) = \frac{P_{\max} \times 100}{I_{sc} \times V_{oc}} = \frac{I_{mp} \times V_{mp}}{I_{sc} \times V_{oc}} \times 100 \quad (19)$$

where P_{max} is the peak power and V_{oc} is the PV open-circuit voltage.

The value of *FF* is always lower than 100%, while the value obtained for non-organic cells is higher than 90% [21].

3. Results and discussions

The PV panel used in the model for validating the current–voltage is a high-efficiency panel called the KC200GT. The electrical characteristics of the two different panels (polycrystalline and monocrystalline) as well as the electrical characteristics calculated using the two-diode circuit models with series and

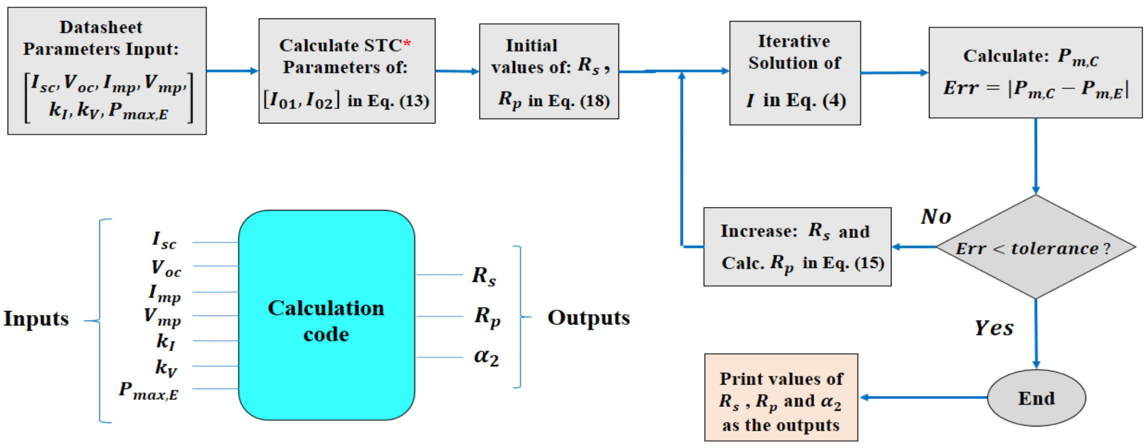

Fig.4. Schematic diagram (left) and detailed view (right) of the MPPM algorithm
STC*: Standard Test Conditions

parallel resistances are shown in Table 1. For the Shell S36 PV panel, in Table 1, the results are compared with those of the model presented in Ref. [9]. Regarding the KC200GT panel, the series resistance with using an error of calculated maximum power with maximum empirical power as minimum ($P_{max,C}$-$P_{max,E}$ < tolerance) is determined at a value of 0.35Ω. Using this series resistance, R_p is equal to 233.69Ω. The $P_{max,C}$ calculated for series resistance of 0.35 is 200.0057W which differs from empirical power by about 0.0057W (*Err*=0.0057W). At this point, the modified α_2 is equal to 1.22. The variations of absolute PV current error in relation to the increase in series resistance is shown in Fig.5.

The most important illustration analyzing the performance of PV cells is obtained from the current–voltage curve as calculated in Eq. (4). The calculated values of series and parallel resistances in circuit analysis of the PV panel for different temperatures and radiations are considered as constant values.

The numerical solution of Eq. (4) results in a voltage–current curve as shown for different temperatures and radiations in Fig.6 and Fig.7, respectively. Eq. (4) is solved numerically for $0 < V < V_{oc}$ and $0 < I < I_{sc}$. As shown in Fig.6, with an increase in radiation, there is a proportionate increase in I_{sc} (owing to an increase in the number of photons which enter the cell causing a proportional number of electrons to separate), while V_{oc} increases a little.

The values of PV current calculated by the circuit model at different voltages varies from the experimental data of temperature and

Table 1. Electrical Characteristics of the different PV panels calculated by the different models in comparison with experimental data, A: The model presented in this paper; B: Datasheet data; and C: The model presented in Ref. [9]

	Monocrystalline		**Polycrystalline**						
	Haeron HR-200W-24/Aab		**Shell S36**			**MSX60**		**KC200GT**	
Parameter	**A**	**B**	**A**	**B**	**C**	**A**	**B**	**A**	**B**
V_{oc} (V)	45.68	45.68	21.4	21.4	21.4	21.1	21.1	32.9	32.9
I_{sc} (A)	5.69	5.69	2.3	2.3	2.3	3.8	3.8	8.21	8.21
V_{mp} (V)	37.88	37.93	16.54	16.5	16.7	17.1	17.1	26.3426	26.3
I_{mp} (A)	5.279	5.27	2.175	2.18	2.16	3.5	3.5	7.5925	7.61
K_I $(A/°C)$	+0.00047	+0.00047	+0.001	+0.001	+0.001	+0.00065	+0.00065	+0.00318	+0.00318
K_V $(V/°C)$	-0.0031	-0.0031	-0.076	-0.076	-0.076	-0.08	-0.08	-0.123	-0.123
N_s	72	72	36	36	36	36	36	54	54
R_s (Ω)	0.40	-	0.9	-	0.89	0.4	-	0.35	-
R_p (Ω)	271.77	-	772.78	-	806.4	259.85	-	233.69	-
α_1	1	-	1	-	1	1	-	1	-
α_2	1.195	-	1.1871	-	NC	1.225	-	1.22	-
I_{ph} (A)	5.698	-	2.303	-	2.3	3.806	-	8.22	-
$P_{max,E}$ (W)	200	200	36	36	36	60	60	200	200
$P_{max,C}$ (W)	200.016	-	35.9745	-	36.072	59.85	-	200.0057	-

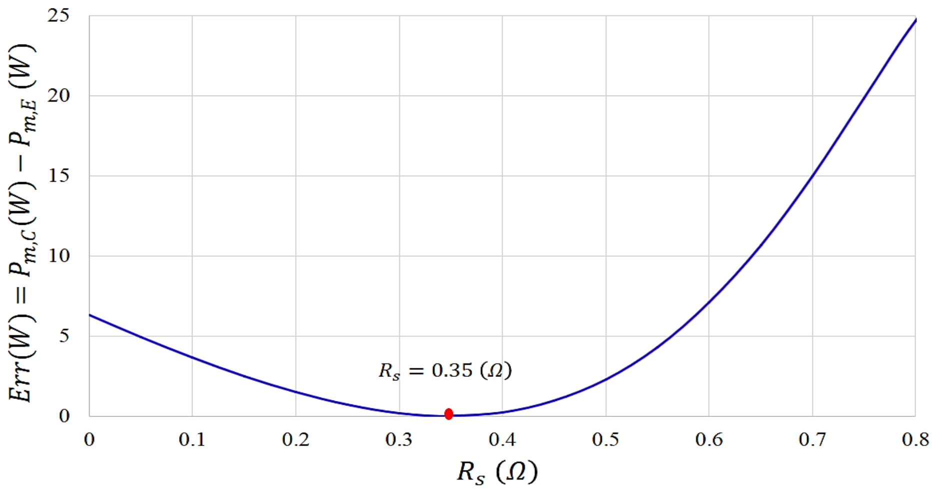

Fig.5. The minimum error between computational and experimental powers at $\alpha_2 = 1.22$

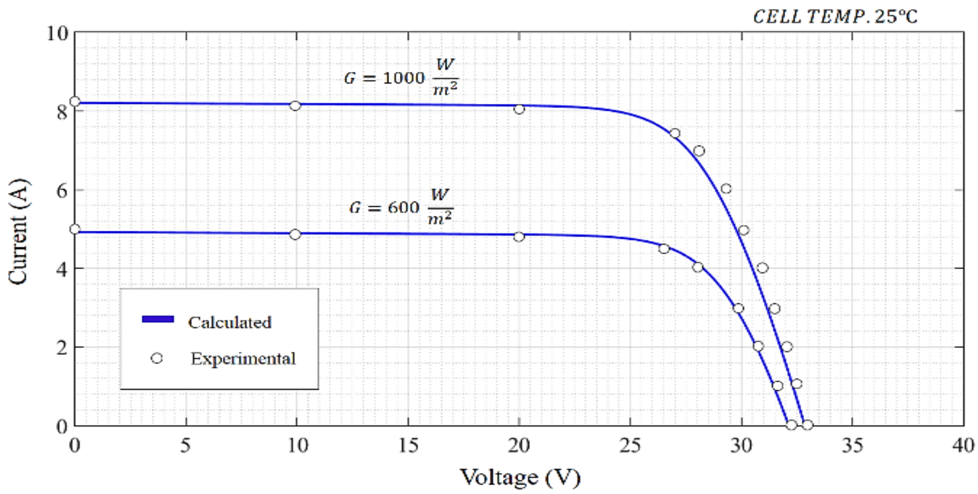

Fig. 6. Current–voltage curves of the KC200GT PV panel for different solar irradiances, *T*=25℃

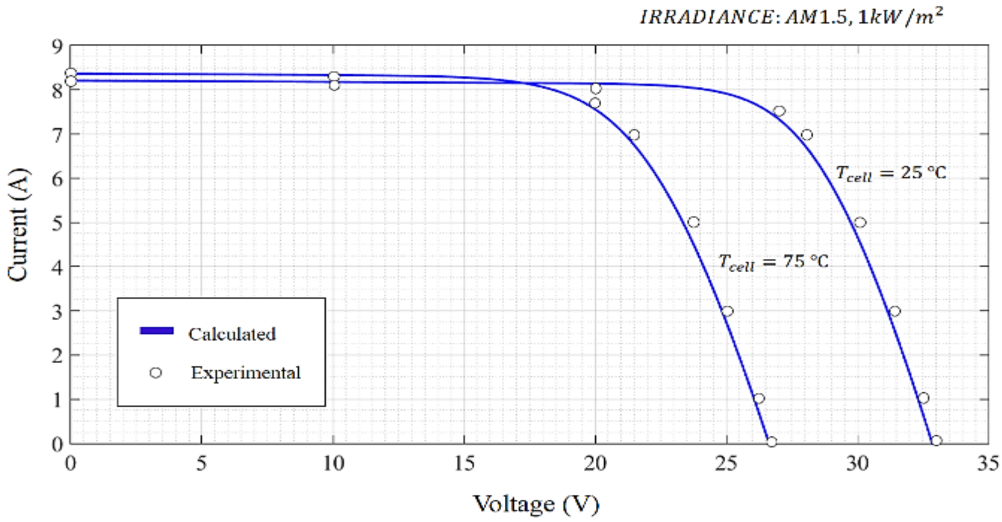

Fig.7. Current–voltage curves of the KC200GT PV panel for different cell temperatures, G=1000$\frac{\mathrm{W}}{\mathrm{m}^2}$

radiation values. The errors of absolute PV current of the model presented in this paper compared with the model presented in Ref. [18] for the KC200GT PV panel at different temperature points are shown in Fig.8 and Fig.9. Table 2 shows the corresponding values of absolute error for the two mentioned models. The mean absolute errors presented in Table 2 for the model proposed in this paper are less than those of Ref. [18] for both given temperatures, which further illustrates the high accuracy of the model. As can be seen in Fig.8 and Fig.9, the absolute PV current errors for the higher voltages are greater in both curves. Due to the sensitivity of PV current to its voltage variations in higher voltages, a small deviation in the voltage and empirical values results in higher deviation of the current. This phenomenon can be seen in all the circuit models which compare calculated values with experimental results [10,22].

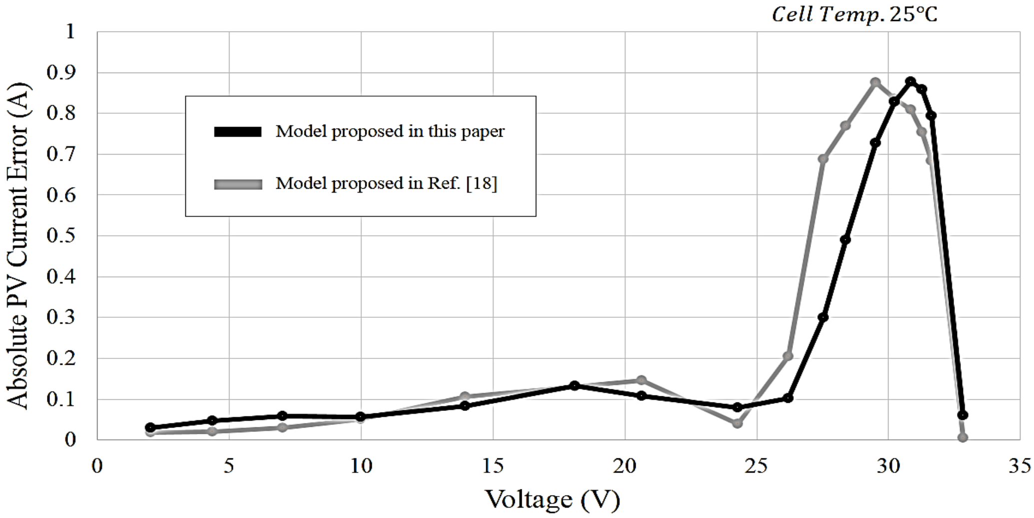

Fig.8. Comparison between absolute PV current errors of the proposed model and Ref. [18] for the KC200GT PV panel at 25℃, G=1000$\frac{\mathrm{W}}{\mathrm{m}^2}$

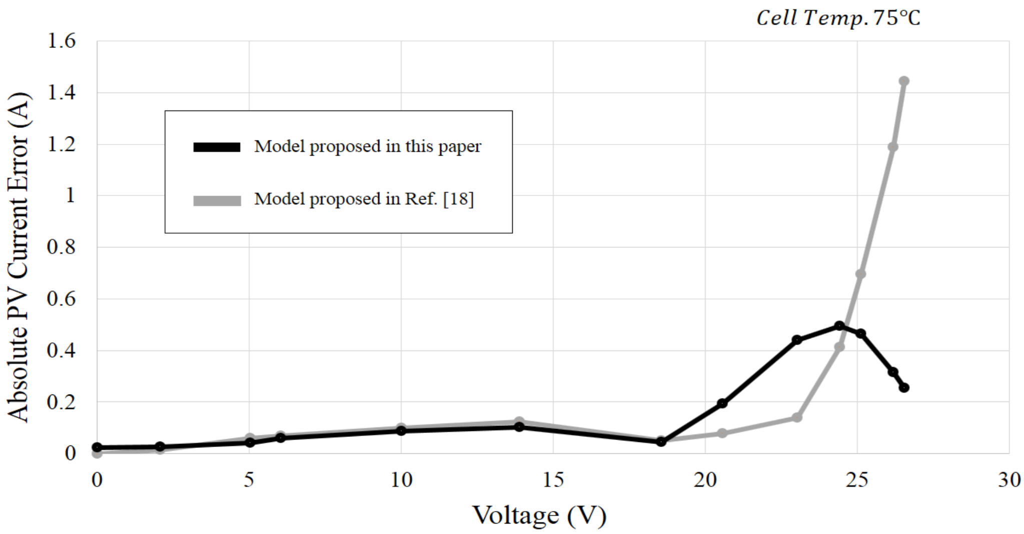

Fig.9. Comparison between absolute PV current error of the proposed model and Ref. [18] for the KC200GT PV panel at 75℃, G=1000$\frac{W}{m^2}$

By determining I and V at each point on the curve, the corresponding power can be easily calculated. The product of I and V at each point gives the output power of the panel. The values of power calculated for different temperatures and radiations are shown in Fig.10 and Fig.11, respectively. As shown in Fig.10, increasing the level of radiation causes $P_{max,C}$ to shift upwards. While an increase in the temperature results in $P_{max,C}$ to occur in low voltages at a slightly reduced value (Fig. 11).

Table 2. Absolute PV current error values at different voltages and mean absolute error for the KC200GT PV panel, A: The model presented in this paper and B: The model proposed in Ref. [18], G=1000$\frac{W}{m^2}$

Voltage (V)		0	4.3	10	14	18.1	20.6	26.2	27.5	29.5	30.8	31.6	**MAE**[1]
Absolute error at 25 °C	A	0.00	0.04	0.05	0.08	0.13	0.11	0.10	0.29	0.72	0.87	0.79	0.2891
	B	0.00	0.02	0.05	0.10	0.13	0.14	0.20	0.68	0.87	0.81	0.68	0.3345
Absolute error at 75 °C	A	0.00	0.04	0.09	0.12	0.01	0.22	0.40	-	-	-	-	0.1257
	B	0.00	0.05	0.10	0.11	0.05	0.07	1.12	-	-	-	-	0.2142

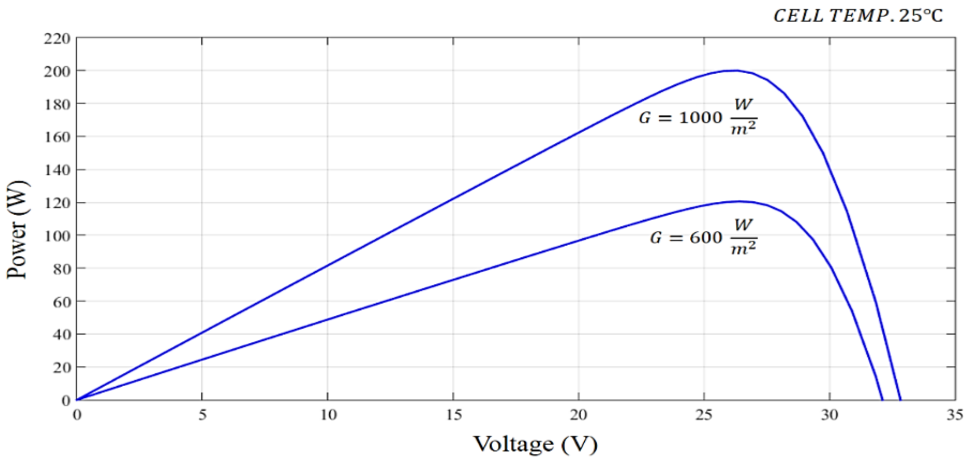

Fig.10. Power-voltage curves of the KC200GT PV panel for different solar irradiances, T=25°C

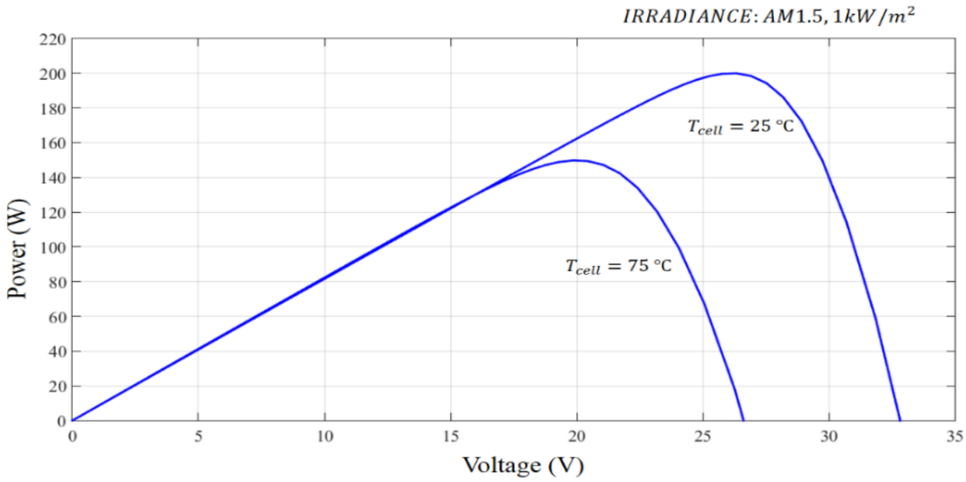

Fig.11. Power-voltage curves of the KC200GT PV panel for different cell temperatures, G=1000 $\frac{W}{m^2}$

[1] Mean Absolute Error

Altering the values of R_s and R_p affects *FF*, considerably. The closer the value of this index to one, higher the quality of the PV cell. The effect of altering the value of R_s on *FF* is shown in Fig.12. According to the datasheet, the value of this index for the KC200GT panel is 74.1%. The value obtained for *FF* at R_s=0.35Ω is 74.1%. By increasing R_s, *FF* is reduced and R_s=0.35Ω, which is its minimum value as shown for the minimum error from FF presented in the datasheet. As R_s increases and moves further away from the desired value, R_p also increases and affects the PV current, thus *FF* increases again moving further away from the value offered in the datasheet.

4.Conclusion

This paper has proposed a two-diode circuit model for calculating the parameters of a PV panel. In order to calculate the parameters of PV panel, the parameters presented in commercial PV datasheets and maximum power point matching (MPPM) algorithm are used. In this work, we calculated the recombination factor of both diodes in a two-diode PV model, to further improve the accuracy of PV model. The ideal factor of Diode1 is assumed to be constant (α_1=1). For the KC200GT panel, R_s and α_2 at which maximum power calculated by the model has a minimum error from experimental power are determined as $\mathbf{0.35\Omega}$ and 1.22, respectively. By increasing R_s gradually, *FF* is reduced and at the series resistance of $\mathbf{0.35\Omega}$, it reaches its minimum error from the value presented in the datasheet. With a further increase in R_s, *FF* increases again and moves further away from the experimental value. The current–voltage curves obtained from the numerical solution of the two-diode model are validated by the experimental data at different temperatures. The absolute errors of the model proposed in this paper are compared with the model proposed in Ref. [18]_for the KC200GT PV panel at two different temperatures ($\mathbf{25}$℃ and $\mathbf{75}$℃). Comparison between these two models showed that the absolute errors at most points of the current–voltage curve in the proposed model are lower than those of the model presented in Ref. [18]. Despite the high accuracy of the model presented in this paper, the error values are fairly high at high voltages. The accuracy of the model, especially at high voltages, may be improved by further reducing the unit of step in iterations of the running code. However, reduction in the unit of steps may considerably increase the running time of the algorithm.

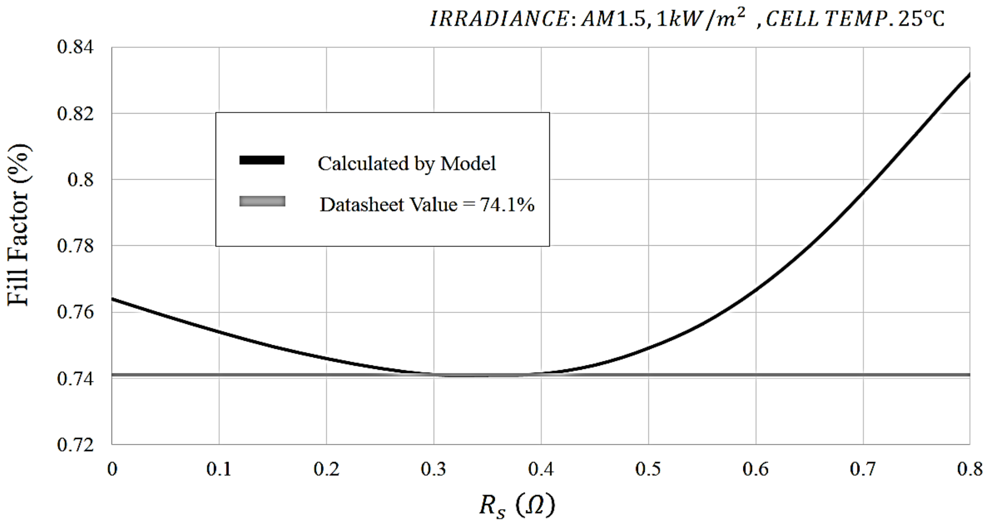

Fig.12. Variations of FF vs. variations of Rs

References

[1] Reis F., Brito M.C., Corregidor V., Wemans J., Sorasio G., Modeling the Performance of Low Concentration Photovoltaic Systems. Solar Energy Materials & Solar Cells (2010) 94: 1222-1226. https://doi.org/10.1016/j.solmat.2010.03.010

[2] Abdulgafar S.A., Omar O.S., Yousif K.M., Improving The Efficiency of Polycrystalline Solar Panel Via Water Immersion Method. International Journal of Innovative Research in Science, Engineering and Technology (2014) 3: 8127-8132.

[3] Anand A., Akella A.K., Modelling and Analysis of Single Diode Photovoltaic Module using MATLAB/Simulink, International Journal of Engineering Research and Applications (2016) 6: 29-34.

[4] Humada A.M., Hojabri M., Mekhilef S., Hamada H.M., Solar Cell Parameters Extraction Based on Single and Double-Diode Models, A Review, Renewable and Sustainable Energy Reviews (2016) 56: 494-509. https://doi.org/10.1016/j.rser.2015.11.051

[5] Lineykin S., Averbukh M. and Kuperman A., An Improved Approach to Extract the Single-Diode Equivalent Circuit Parameters of a Photovoltaic Cell/Panel, Renewable and Sustainable Energy Reviews (2014) 30: 282-289. https://doi.org/10.1016/j.rser.2013.10.015

[6] Tamrakar V., Gupta S.C., Sawle Y., Single-Diode PV Cell Modeling and Study of Characteristics of Single and Two-Diode Equivalent Circuit. Electrical and Electronics Engineering, An International Journal (2015) 4: 13-24. https://doi.org/ 10.14810/elelij.2015.4302

[7] Masters G.M., Renewable and Efficient Electric Power Systems. John Wiley & Sons, New Jersey (2004).

[8] Martin A.G., Third Generation Photovoltaics, Solar Cells for 2020 and Beyond, Physica E (2002) 14: 65-70. https://doi.org/10.1016/S1386-9477(02)00361-2

[9] Ishaque K., Salam Z., Taheri H., Accurate MATLAB Simulink PV System Simulator Based on a Two-Diode Model, Journal of Power and Electronics (2011) 11: 179-187. https://doi.org/10.6113/JPE.2011.11.2.179

[10] Villalva M.G., Gazoli J.R., Filho E.R., Comprehensive Approach to Modeling and Simulation of Photovoltaic Arrays. IEEE Transactions on Power Electronics (2009) 24: 1198-1208. https://doi.org/10.1109/TPEL.2009.2013862

[11] Bikaneria J., Joshi S.P., Modelling and Simulation of PV Cell Based on Two-Diode Model. Int. J. of Recent Trends in Engineering & Technology (2014) 11: 589-594. https://doi.org/10.1016/j.egypro.2015.07.822

[12] Carrero C., Amador J., Arnaltes S., A Single Procedure for Helping PV Designers to Select Silicon PV Modules and Evaluate the Loss Resistances, Renewable Energy (2007) 32: 2579-2589. https://doi.org/10.1016/j.renene.2007.01.001

[13] Azzouzi M., Popescu D., Bouchahdane M., Modeling of Electrical Characteristics of Photovoltaic Cell Considering Single-Diode Model. Journal of Clean Energy Technologies (2016) 4: 414-419. https://doi.org/10.18178/JOCET.2016.4.6.323

[14] Ma J., Man K.L., Ting T.O., Zhang N., Approximate Single-Diode Photovoltaic Model for Efficient *I-V* Characteristics Estimation. The Scientific World Journal (2013) 2013: 1-7. http://dx.doi.org/10.1155/2013/230471

[15] Laudani A., Fulginei F.R. and Salvini A., High Performing Extraction Procedure for the One-Diode Model of a Photovoltaic Panel from Experimental I–V Curves by Using Reduced Forms, Solar Energy (2014) 103: 316-326. https://doi.org/10.1016/j.solener.2014.02.014

[16] Chan D.S.H., Phang J.C.H., Analytical Methods for the Extraction of Solar-Cell Single- and Double-Diode Model Parameters from I- V Characteristics. IEEE Transactions on Electron Devices (1987) 34: 286-293. https://doi.org/10.1109/T-ED.1987.22920

[17] Kou Q., Klein S.A., Beckman W.A., A Method for Estimating the Long-Term Performance of Direct-Coupled PV

Pumping Systems. Solar Energy (1998) 64: 33-40. https://doi.org/10.1016/S0038-092X(98)00049-8

[18] Walker G., Evaluating MPPT Converter Topologies Using a Matlab PV Model. Journal of Electrical and Electronic Engineering Australia (2001) 21: 45–55.

[19] Ciulla G., Brano V.L., Moreci E., Forecasting the Cell Temperature of PV Modules with an Adaptive System. International Journal of Photoenergy (2013) 2013: 1-10. http://dx.doi.org/10.1155/2013/192854

[20] Ahmad T., Sobhan S., Nayan Md.F., Comparative Analysis between Single Diode and Double Diode Model of PV Cell: Concentrate Different Parameters Effect on Its Efficiency, Journal of Power and Energy Engineering (2016) 4: 31-46. https://dx.doi.org/10.4236/jpee.2016.43004

[21] Qi B., Wang J., Fill Factor in Organic Solar Cells, Physical Chemistry Chemical Physics (2013) 15: 8972-8981. https://doi.org/10.1039/C3CP51383A

[22] Dehghanzadeh A., Farahani G., Maboodi M., A Novel Approximate Explicit Double-Diode Model of Solar Cells for Use in Simulation Studies. Renewable Energy (2017) 103: 468-477. https://doi.org/10.1016/j.renene.2016.11.051.